Proceedings of the Korean Nuclear Society Spring Meeting
Yongpyung, Korea, Oct. 2002

Evaluation of Neutron Emission Spectra from Proton-Induced Reaction for Space Shielding

Young-Ouk Lee and Jonghwa Chang

Korea Atomic Energy Research Institute
P.O. Box 105 Yusong, Taejon 305-600, Korea

Myung-Hyun Kim

Kyunghee University
Yong-In, 449-701, Korea

Abstract

Neutron contribution is an important component of the secondary radiation field. For energies up to 400 MeV encompassing most of the incident spectrum for trapped protons and solar energetic particle events, energy-angle spectra of secondary neutrons produced from the proton-induced neutron production reaction are evaluated using the optical model for the direct reactions, Hauser-Feshbach model for the equilibrium emission, and exciton model for the preeqilibrium emission, based on selected reference measrements. As a result, a good agreement has been achieved for entire emission energy and angle range, except for slight discrepancies at preequilibrium emission energies.

I. Introduction

Calculation of space system shielding is complicated due to the production of secondary products. Among the secondary nucleons, neutron penetration has entirely different nature compared to that of charged particles. While the secondary proton dose is mainly due to the large number of low energy protons produced in the shielding immediately adjacent to the dose point, a large fraction of the neutrons produced through the whole shield may be transported to the dose point. Thus, neutron contribution is an important component of the secondary radiation field, especially for astronauts protected by thick shielding on lunar or Martian bases.

Most computer codes for space radiation shielding have an empirical formula for proton-nucleus non-elastic cross sections and neutron emission spectra based on the Bertini's intra-nuclear-cascade (INC) model [1] for the secondary neutron production spectra in the shielding materials for energies up to a few GeV of incident protons.

Recently, however, more rigorous models have been applied to provide nucleon-nucleus reaction data for energies below a few hundred MeV where underlying physical assumptions of the INC model are not well satisfied. As an example of such efforts, Los Alamos evaluation library (LA150) [2] contains neutron- and proton-induced nuclear reaction data for approximately 30 important isotopes for energies below 150 MeV. For energies up to 400 MeV encompassing most of the incident spectrum for trapped protons and solar energetic particle events, proton-nucleus non-elastic cross sections were evaluated [3] using an energy-dependent optical model with accumulated measurements. On the other hand, the Galactic Cosmic Ray (GCR) protons spectrum, whose energies are higher than 400 MeV, is also important for the shielding of secondary neutrons in the thick shields that can be used in Martian or Lunar bases.

The present work extends previous proton-nucleus non-elastic cross sections [3]. Energy-angle spectra of secondary neutrons produced from the proton-induced neutron production reaction, symbolized as (p, xn), of ^{27}Al and ^{208}Pb for energies below 400 MeV are evaluated based upon model calculations guided and benchmarked by existing experimental data. Since nuclear interactions are more sensitive to specific details of nuclear structure along with quantum effects for energies below few hundred MeV, our theoretical evaluation uses the optical model for the direct reactions, Hauser-Feshbach model for the equilibrium emission, and exciton model for the preeqilibrium emission.

Computation time of our model calculation is much shorter than the INC models which use Monte Carlo methods. Typical computation time varies according to the excitation energy and target mass; it takes a few minutes for light nuclei such as aluminim, and several hours for heavy nuclei such as lead on a Pentium-III PC.

II. Reference Measurements

Most of the measurements for energies below 150 MeV referenced in the LA150 library evaluation were also adopted in the present evaluation, and details are found in [3, 4]. Additionally, important measurements of neutron emission spectra above 100 MeV of incident proton energy are referenced in Meier [5, 6], Scobel [7], and Stamer [8]. These four sets of measurements, listed in Table 1, provided important guidances in evaluating energy-angle spectra of emitted neutron for energies above 150 MeV.

For the ^{27}Al case, Meier's measurements for 113 MeV protons [5], Scobel's measurements for 160.3 MeV protons [7], and Stamer's [8] and Meier's measurements [6] for 256 MeV were referenced. It was reported in the references that the INC evaporation calculations using the High Energy Transport Code (HETC) showed good agreements at 30 and 60 degrees, but the discrepancies at 7.5 and 150 degrees are as much as a factor of 7.

For the ^{208}Pb case, we referred to Scobel's measurements for 120 and 160.3 MeV protons [7] and Stamer's [8] and Meier's measurements [6] for 256 MeV protons. In the cases of 120 and 160.3 MeV, it was reported that the measurements are well reproduced by the phenomenological parameterization of Kalbach [9]. However, for the 256 MeV cases, the Meier [6] showed poor agreements between the data and the HETC calculation especially for very forward and backward angles, and Stamer et al. [8] reported that the INC model of Bertini underestimated the magnitudes of neutron production at 120 and 150 deg.

Electronic versions of all the measured data were retrieved from the Exchange File Format (EXFOR) database at Nuclear Energy Agency (NEA) [10] and their integrities were checked. It is found that the Stamer's EXFOR data for 256 MeV protons (EXFOR entries C0511.004 and C0511.008) contain neutron emission data of energies below 20 MeV, which were not presented in the publication [8]. Since the paper noted that the experimental spectra obtained are almost exclusively attributable to a preequilibrium emission mechanism, and the energy resolution of the detectors are from 16 to 29 MeV in the experiments, the data below 20 MeV from the EXFOR were excluded from our reference measurements.

III. Theoretical Models

1. Optical Models

The optical model supplies not only the non-elastic cross section and the angular distribution of elastic scattering, but also the particle transmission coefficients for emission model

Table 1: Reference measurements of neutron double-differential emission spectra for incident proton energy above 100 MeV

Reaction	Principal Author	E_p [MeV]	Emission Angles [deg]	EXFOR entry
$^{27}Al(p,xn)$	Meier [5]	113.0	7.5, 30, 60, 150	O0100
	Scobel [7]	160.3	0 - 145 (14 angles)	O0181
	Stamer [8]	256.0	7.5, 30, 60, 150	C0511
	Meier [6]	256.0	7.5, 30, 60, 150	C0168
$^{208}Pb(p,xn)$	Scobel [7]	120.0	0 - 145 (14 angles)	O0181
	Scobel [7]	160.3	0 - 145 (14 angles)	O0181
	Stamer [8]	256.0	7.5, 30, 60, 150	C0511
$^{nat}Pb(p,xn)$	Meier [6]	256.0	7.5, 30, 60, 150	C0168

calculations, such as equilibrium and preequilibrium decay models. In this work, the energy dependent potential wells for neutrons and protons were adopted from the previous work of Korea Atomic Energy Research Institute (KAERI) high energy library evaluation task [3, 4] for particle energies up to 400 MeV. Figure 1 shows proton-nucleus non-elastic cross sections and angular distribution of elastic scattering for both ^{27}Al and ^{208}Pb, resulting from the optical model analysis. The proton-nucleus non-elatic cross section $\sigma_r(E)$ is directly related to the energy-angle spectra of secondary neutrons ($\sigma_{xn}(\mu, E, E'$) as:

$$\sigma_{xn}(\mu, E, E') = \sigma_r(E) y_n(E) f_n(E, E', \mu)/2\pi \quad (1)$$

where E is the incident energy, E' is the energy of the neutron emitted with cosine μ, $y_n(E)$ is the neutron yield, and $f_n(E, E', \mu)$ is the normalized energy-angle distribtion of emitted neutron.

2. Emission Models

For the emission reaction the latest version of the GNASH code [11] has been used. The GNASH treats a nuclear reaction as proceeding through an initial preequlibrium phase, from which high-energy ejectiles can be emitted, followed by a process of sequential particle emission from decaying compound nuclei, until the final residual nucleus attains its ground state via particle or gamma-ray emission. The Hauser-Feshbach theory is used to calculate emission from the compound nucleus, with a full conservation of spin and parity. Production cross sections and emission spectra of secondary light particles, gamma-rays, and recoil nuclides are obtained from the calculations.

For such calculations in the GNASH code, several models and parameters are needed such as optical model transmission coefficients, gamma-ray transmission coefficients, level density models, preequilibrium components, and direct reaction effects. The transmission coefficients were provided by the optical model analysis. The file of discrete level information and ground-state masses, spin and parities was provided [12]. The mass values were based upon the 1995 Audi compilation [13], and in the case of unmeasured masses, the values from the Moeller and Nix calculations [14] were supplemented. The Ignatyuk [15] nuclear level densities were used for describing the statistical level density properties of excited nuclei. It utilizes an energy dependent level density parameter to wash out the effects of shell closures for nuclei near closed shells at higher energies.

Since many different residual nuclei can be produced in nuclear reactions up to 400 MeV, a limited number of low-lying discrete levels were used and the statistical level densities were matched continuously onto the density of known low-lying levels.

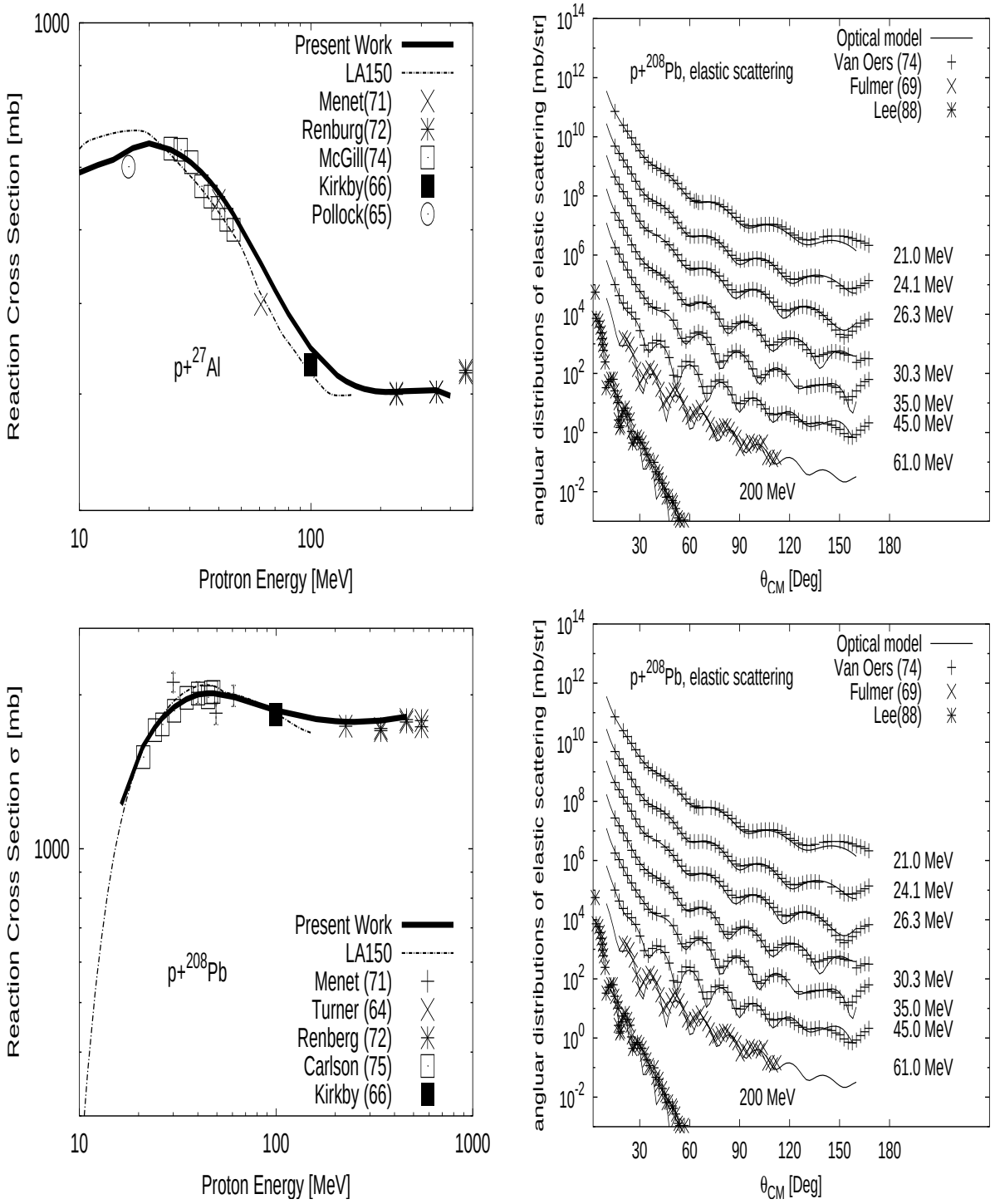

Figure 1: Reaction cross sections (Left) and elastic scattering angular distributions (right) for ^{27}Al and ^{208}Pb obtained from the optical model analysis for proton energies up to 400 MeV. The elastic scattering data of p+^{27}Al for 17.0 MeV, 28.8 MeV ..., were shifted by a factor of 10^4, 10^3, ..., espectively. The elastic scattering data of p+^{208}Pb for 21.0 MeV, 24.1 MeV ..., were shifted by a factor of 10^7, 10^6, ..., respectively.

The GNASH code has the exciton model in combination with the Kalbach angular-distribution systematics [9] to describe the processes of preequilibrium emission, and damping to equilibrium, during the evolution of the reaction. In the GNASH code, a simplified preequilibrium expression based upon the exciton model has been used to correct reaction and level-excitation cross sections as well as spectra for preequilibrium effects :

$$\left(\frac{d\sigma}{d\epsilon}\right)_{preq} \propto \frac{\sigma_{\rm inv}(\epsilon) m \epsilon \sigma_R}{|M|^2 g^4 E^3} \sum_{n=3}^{\bar{n}} (U/E)^{n-2}(n+1)^2(n-1), \tag{2}$$

where E and U are the excitation energies of the compound and residual nuclei, respectively; σ_R is the incident particle non-elastic cross section; m, ϵ, and $\sigma_{inv}(\epsilon)$ are the mass, kinetic energy, and inverse cross section for the outgoing particle; g is the average single-particle level spacing from the Fermi-gas model; and n is the number of particles and holes ($n = p + h$) in the compound nucleus. The sum extends from the initial exciton number 3 to $\bar{(n)}$, the limiting value attained when equilibrium is reached. To achieve a global agreement with the emission spectra measurements, the absolute square of the damping matrix $|M|^2$ has been tuned as a phenenological fudge factor.

The pion production channel opens at its production threshold energy (around 150 MeV), but the present model calculation deos not include the pion channel, because its emission fraction to that of neutrons is at most 1 % at the higher emission energies for the energy range of our interest (see [16]).

IV. Results and Comparisons

In order to give an overview of our evaluation results, Figure 2 provides 3-dimensional plots of the angle-integrated emission spectra information of neutrons. These plots, for protons incident on ^{27}Al and ^{208}Pb, are products of non-elastic cross sections, multiplicities (yields), and angle-integrated energy distributions that were evaluated in the present work expressed as an angle-integral of equation (1):

$$\sigma_{xn}(E, E') = \sigma_r(E) y_n(E) \int d\mu f_n(E, E', \mu)/2\pi \tag{3}$$

It shows the trends of increasing high-energy preequilibrium emission with increasing incident proton energy.

1. ^{27}Al

Figure 3 shows a comparison of our evaluation, the LA150 library, and the measurements of Meier [5] for double-differential neutron emission spectra at 7.4, 30, 60 and 150 degrees for incident protons of 113 MeV. Agreement is fairly good over the whole range of emission energies and angles except for slight overestimations for neutron energies below 20 MeV.

For incident proton energies above 150 MeV, our evaluations are compared in Figure 4 with the measurements of Scobel [7] for 160.3 MeV and in Figure 5 with the measurements of Stamer [8] for 256 MeV. Good agreements are shown in Figure 4 for the 160.3 MeV case except at 145 degree, where our model calculations underestimate the measured neutron spectra. However, this descrepancies do not appear to be systematic in our model calculations since we have good agreements at 150 degree of 113 MeV and 256 MeV protons (see Figs. 3 and 5).

The 256 MeV case in Figure 5 gives reasonable agreements except for slight overestimations at higher emission energies (preequilibrim emission) at 7.5 degree. The magnitude of the calculated

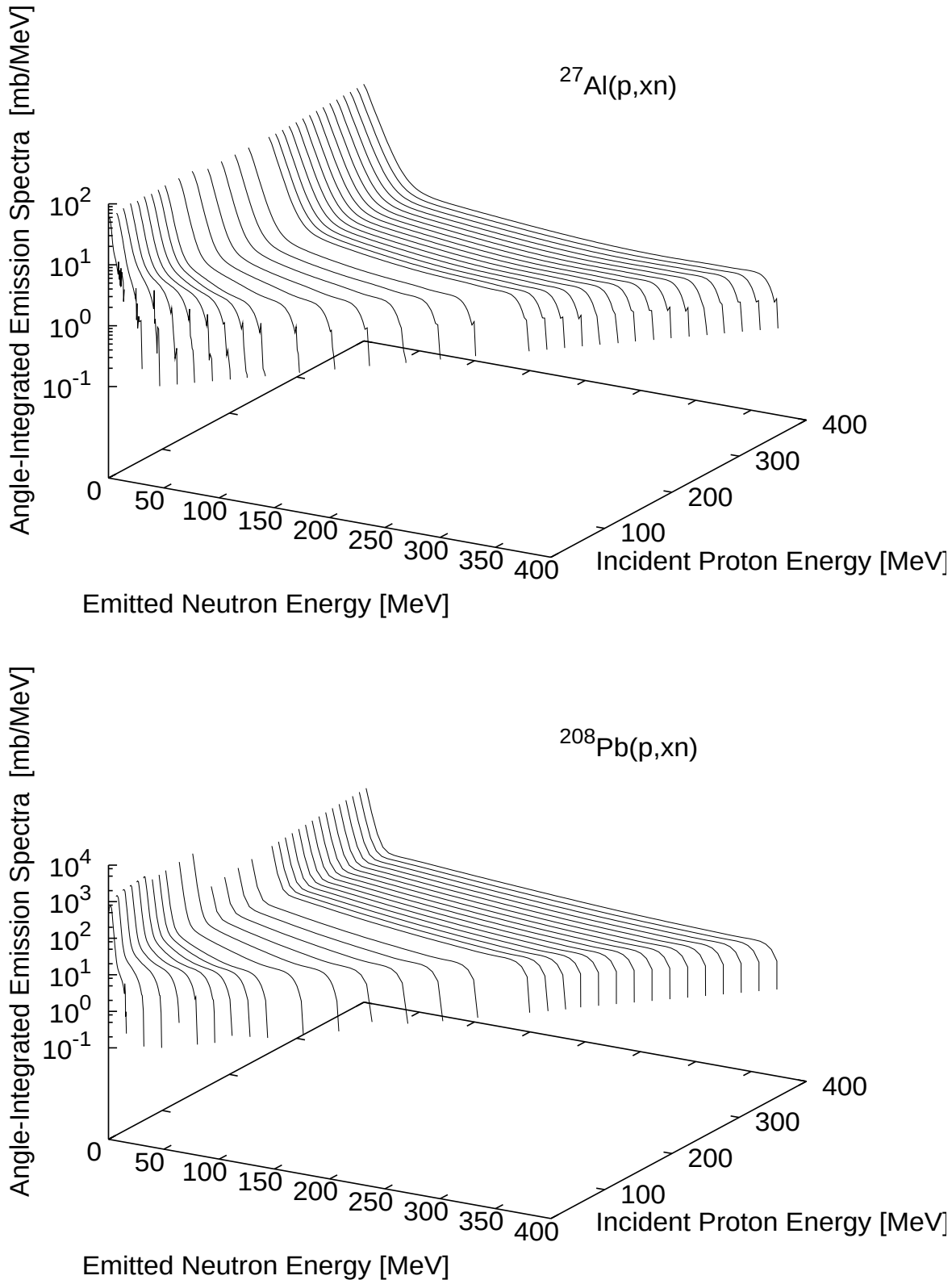

Figure 2: Evaluated angle-integrated neutron emission spectra for ^{27}Al and ^{208}Pb reactions

preequilibrium emission spectra is determined by the Kalbach angular-distribution systematics in the GNASH code, and its accuracy is within that of of the Kalbach systematics.

2. ^{208}Pb

Figure 6 shows a comparison of our evaluation, the LA150 library, and the measurements of Scobel. [5] for double-differential neutron emission spectra at 11, 45, 95 and 145 degrees for incident protons of 120 MeV. Agreement is fairly good over the whole emission energies and angles except at 145 degree, where our model calculations as well as the LA150 library are smaller than the measured data. Again, this descrepancies do not appear to be systematic in our model calculations since we have good agreements at 145 degree of 160 MeV and at 150 degree of 256 MeV protons (see Fig. 7 and 8).

For incident proton energies above 150 MeV, our evaluations are compared in Figure 7 with the measurements of Scobel [7] for 160.3 MeV, and in Figure 8 with the measurements of Meier [6] and Stamer [8] for 256 MeV. While good agreements are shown for the 160.3 MeV case, the 256 MeV case gives reasonable agreements except for for slight overestimations at emission energies between 15 and 50 MeV, which is due to the limitation of Kalbach angular-distribution systematics.

V. Conclusion

Below 150 MeV of incident protons, no significant differences are noticed between our evaluation and the LA150 library, giving a good consistency with the measurements. This is mainly because the reference measurements, theoretical models, and model parameters are nearly the same for our evaluation and the LA150 library except the transmissition coefficients of neutrons and protons, whose effects are minimal in the inclusive emission spectra.

For energies between 150 and 400 MeV, our evaluations are made on the same reaction models as the LA150 library, but with

- utilization of the optical model parameters of neutrons and protons validated for incident energies up to 400 MeV,
- benchmark with appropriate reference measurements for energies above 150 MeV, and
- adjustment of absolute square of the damping matrix to have a global agreement with emission spectra.

As a result, fairly good agreement has been achieved in the neutron double differential emission spectra for entire emission energy and angle range. Slight discrepancies are observed at preequilibrium emission energies between 15 and 50 MeV for 256 MeV protons incident on ^{208}Pb, which come from the limitation of Kalbach angular-distribution systematics.

Acknowledgments

This work was supported by the Korea Science and Engineering Foundation and the Korea Ministry of Science and Technology.

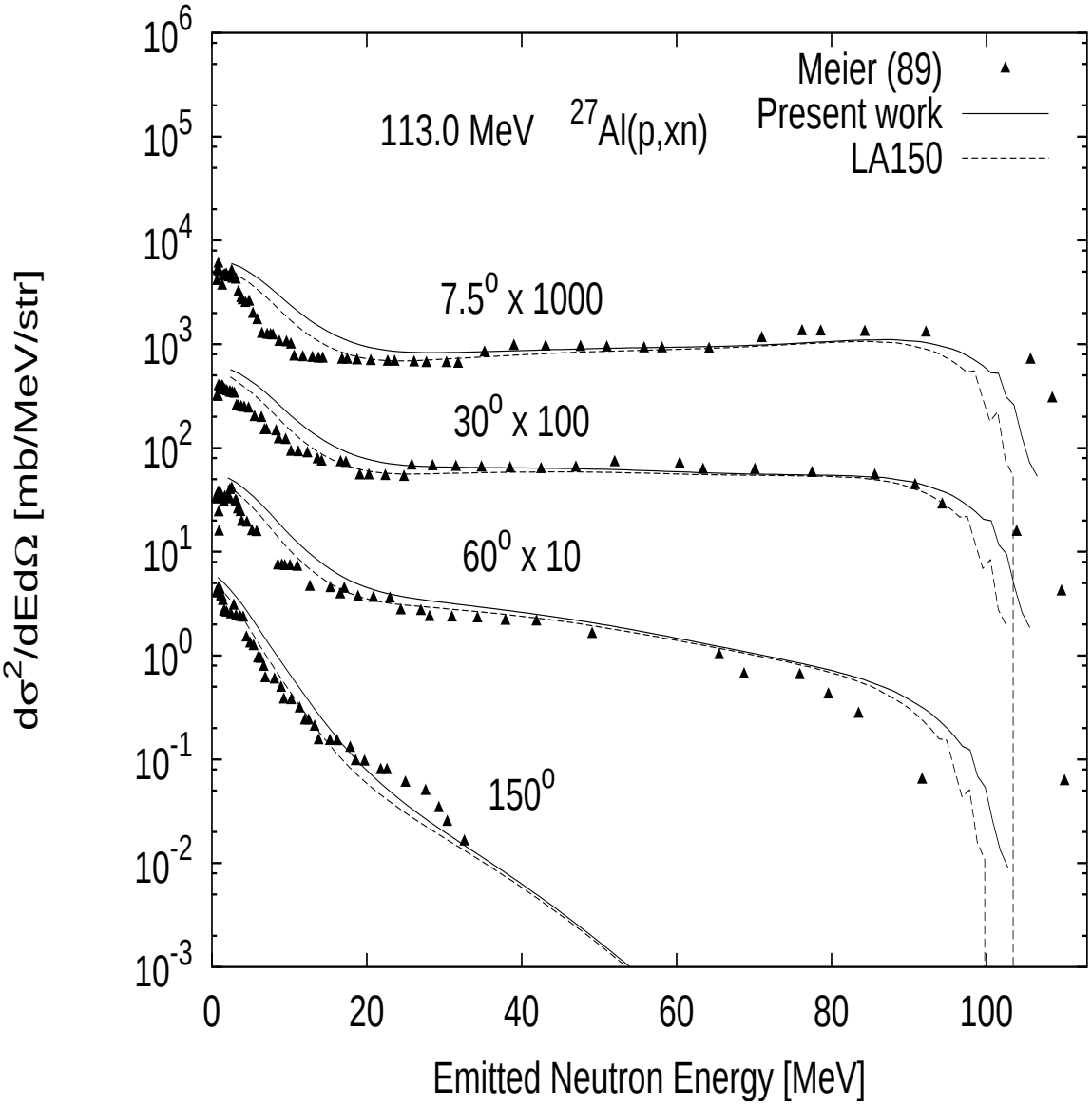

Figure 3: Evaluated $^{27}\mathrm{Al}(p, xn)$ double-differential neutron emission spectra compared with experimental data and the LA150 library at 113 MeV incident energy. Note that the data for 7.5, 30 and 60 degrees were multiplied by 1000, 100 and 10 respectively for clarity of presentation.

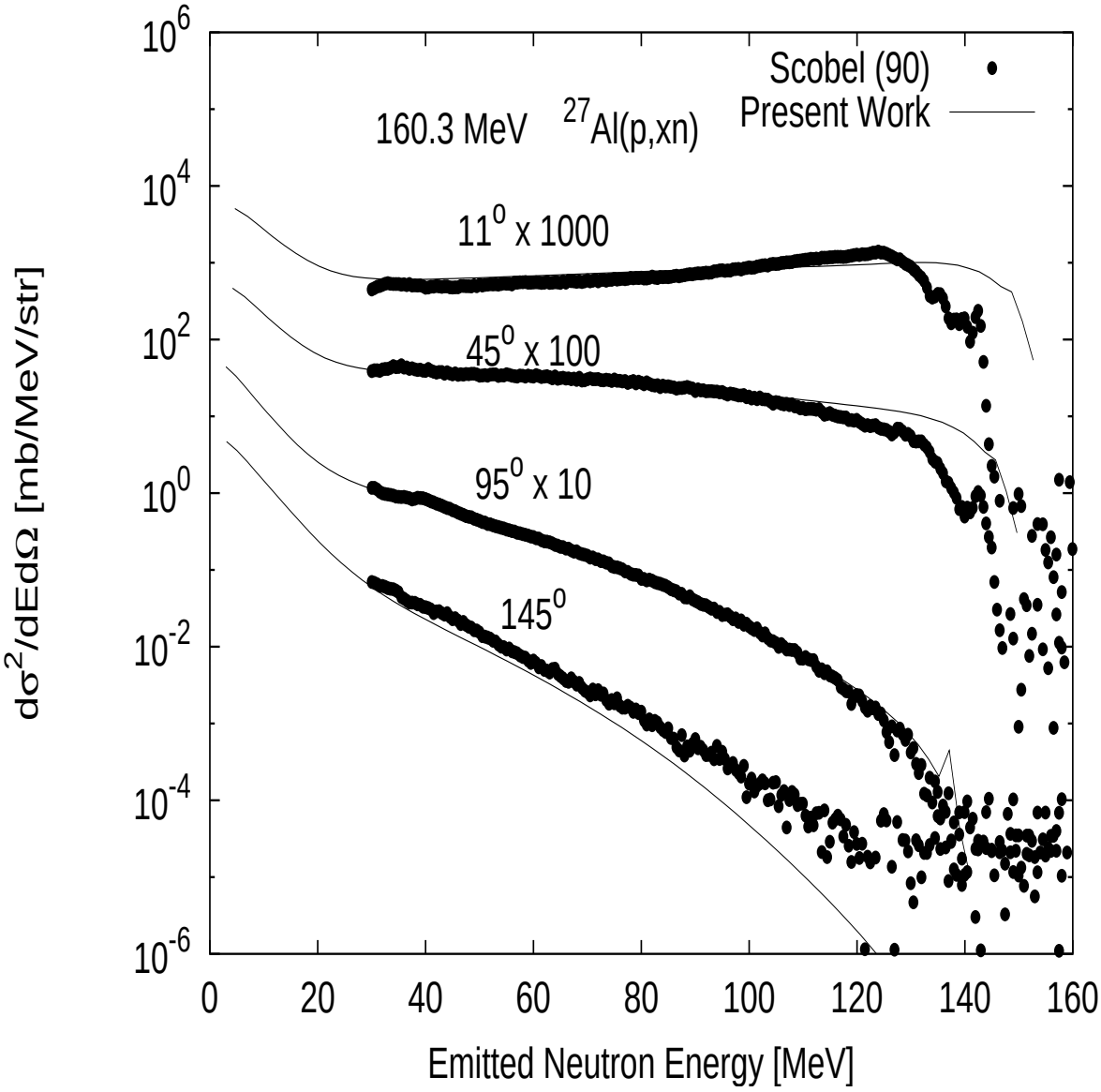

Figure 4: Evaluated $^{27}\mathrm{Al}(p, xn)$ double-differential neutron emission spectra compared with experimental data at 160.3 MeV incident energy. Note that the data for 11, 45 and 95 degrees were multiplied by 1000, 100 and 10 respectively for clarity of presentation.

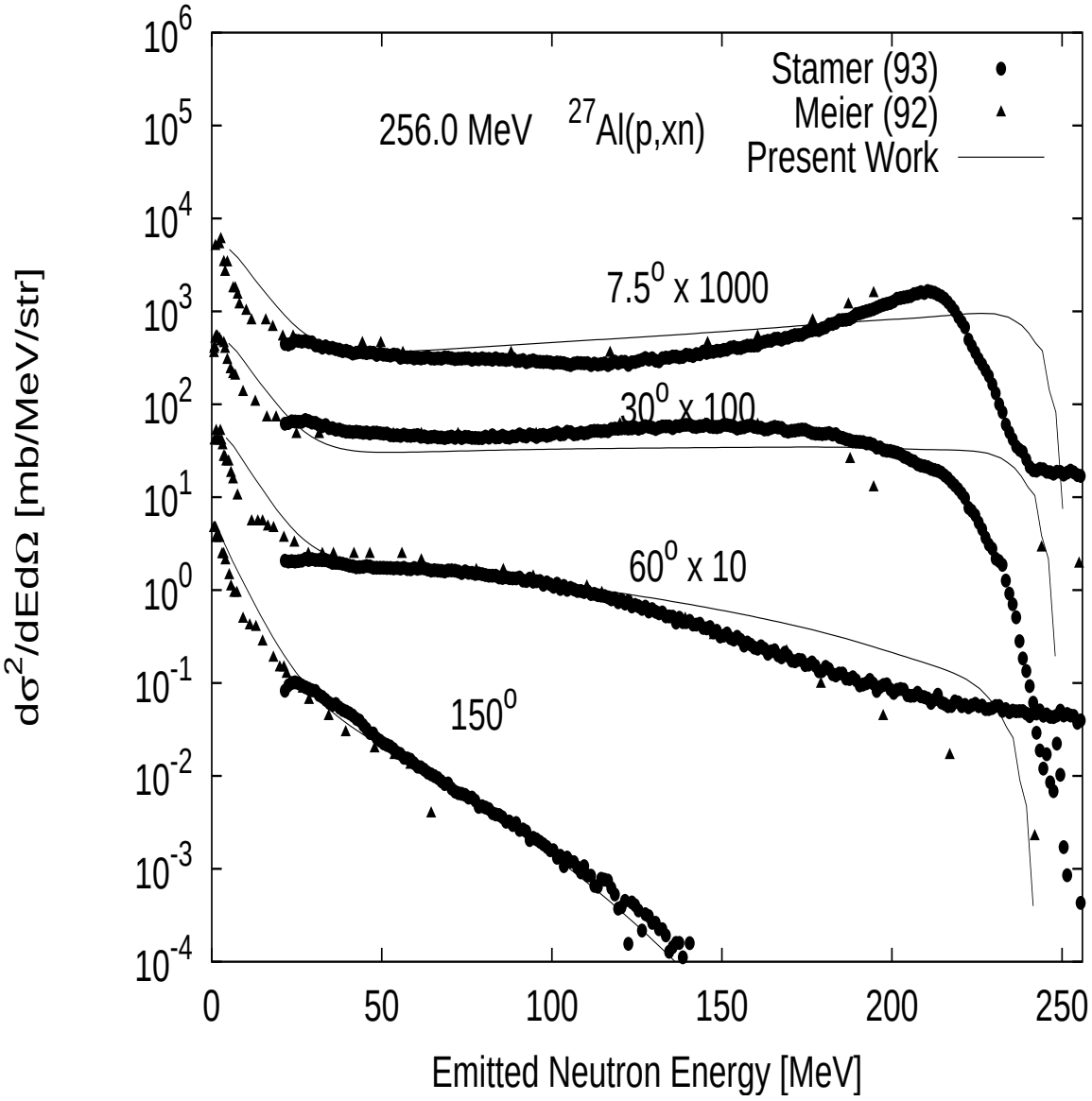

Figure 5: Evaluated $^{27}\mathrm{Al}(p, xn)$ double-differential neutron emission spectra compared with experimental data at 256 MeV incident energy. Note that the data for 7.5, 30 and 60 degrees were multiplied by 1000, 100 and 10 respectively for clarity of presentation.

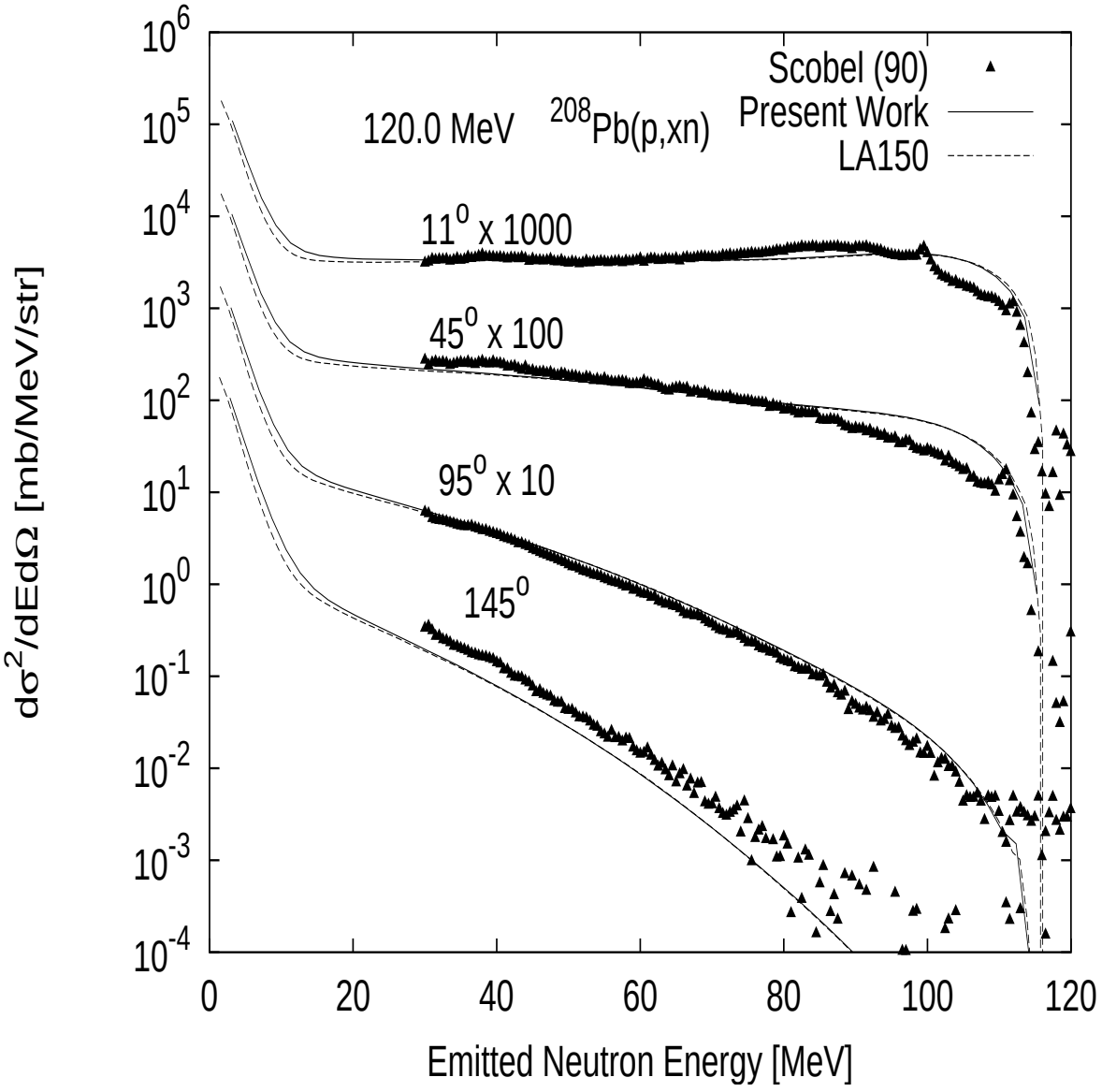

Figure 6: Evaluated $^{208}\mathrm{Pb}(p, xn)$ double-differential neutron emission spectra compared with experimental data and the LA150 library at 120 MeV incident energy. Note that the data for 11, 45 and 95 degrees were multiplied by 1000, 100 and 10 respectively for clarity of presentation.

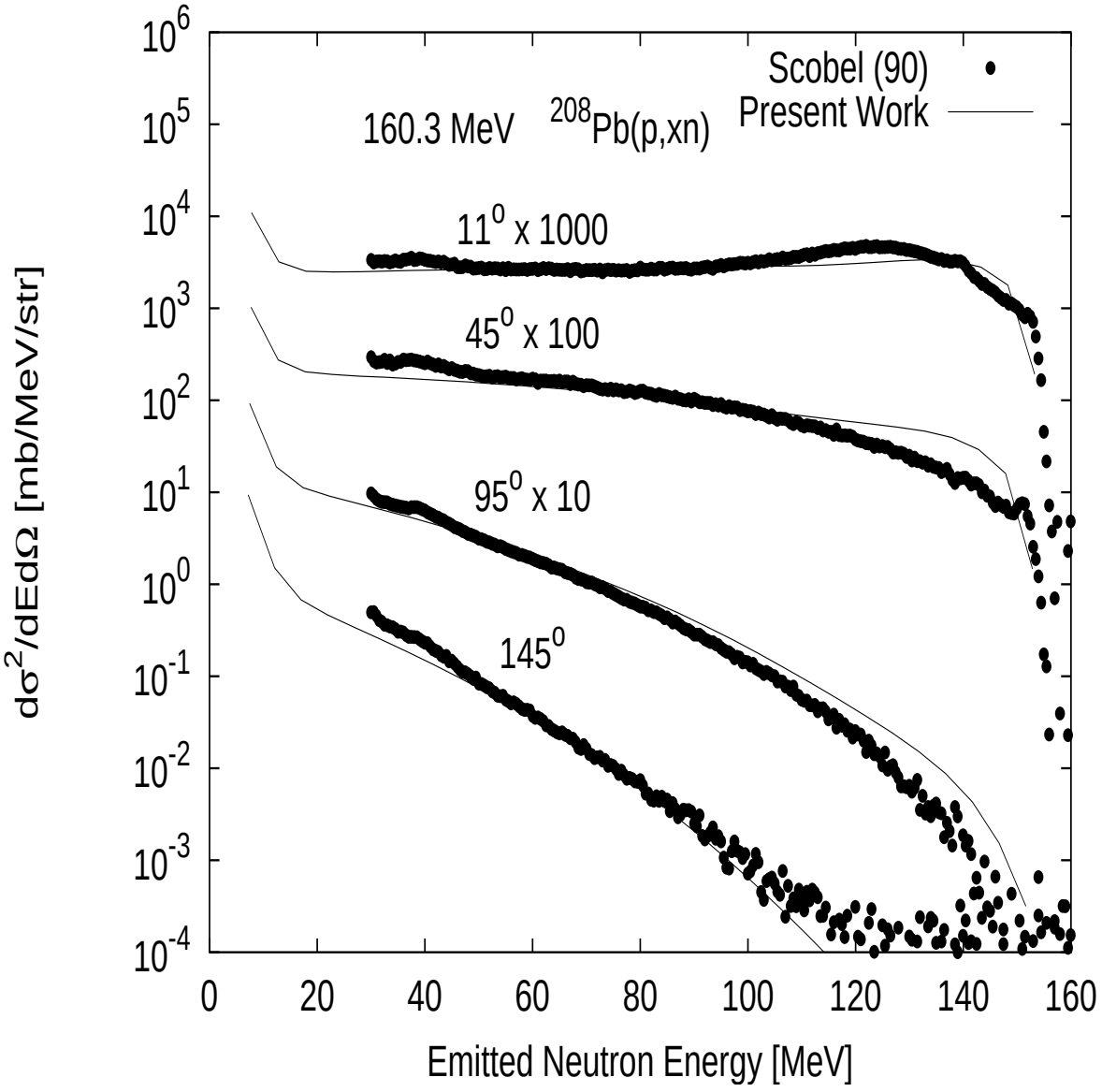

Figure 7: Evaluated ^{208}Pb(p, xn) double-differential neutron emission spectra compared with experimental data at 160.3 MeV incident energy. Note that the data for 11, 45 and 95 degrees were multiplied by 1000, 100 and 10 respectively for clarity of presentation.

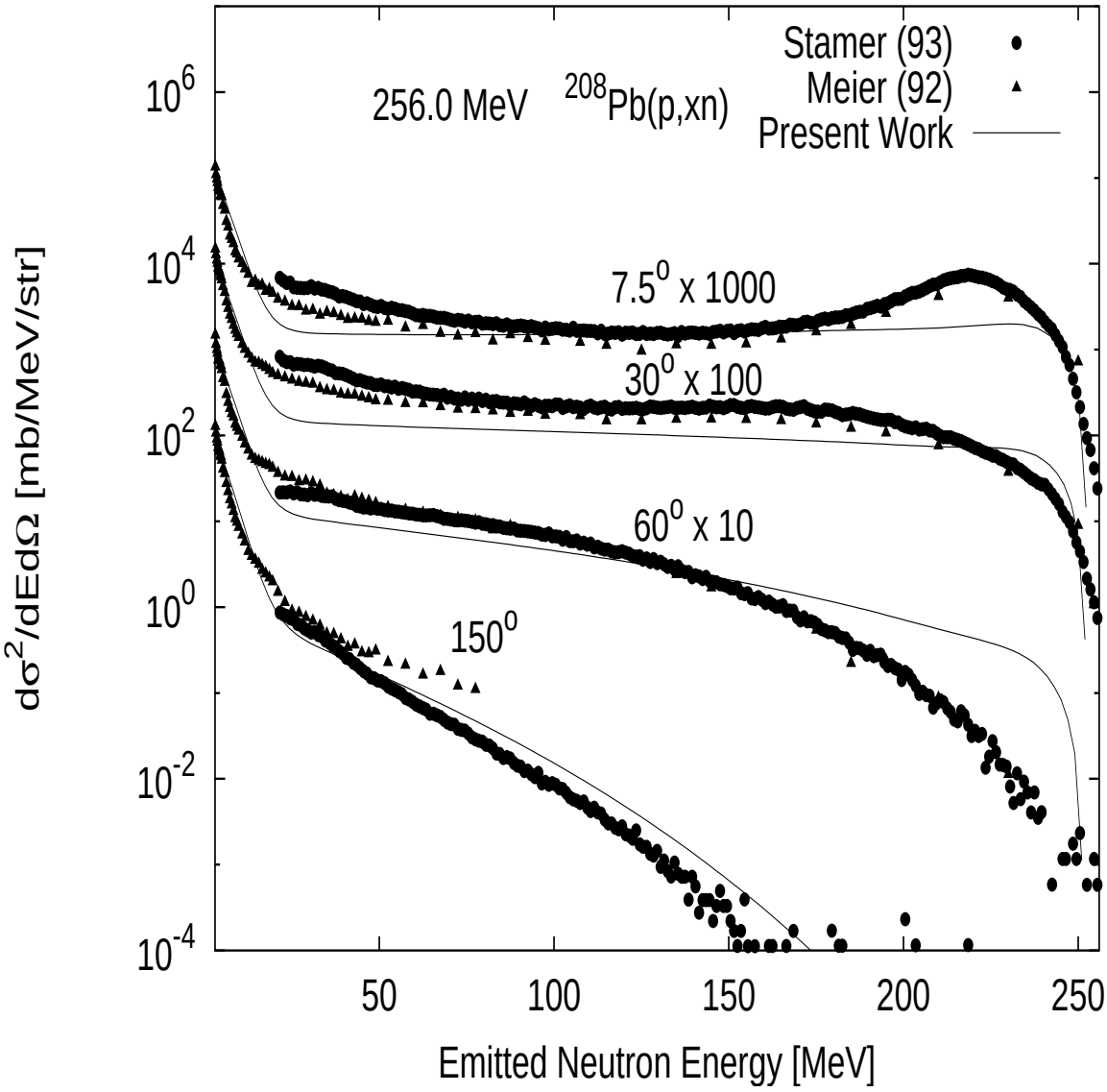

Figure 8: Evaluated ^{208}Pb(p, xn) double-differential neutron emission spectra compared with experimental data at 256 MeV incident energy. Note that the data for 7.5, 30 and 60 degrees were multiplied by 1000, 100 and 10 respectively for clarity of presentation.

References

[1] H. W. Bertini, "Intranuclear-cascade calculation of the secondary nucleon spectra from nucleon-nucleus interactions in the energy range 340 to 2900 MeV and comparisons with experiment," *Phys. Rev.*, vol. 188, pp. 1711–1730, 1969.

[2] M. Chadwick and et al., "Cross section evaluations to 150 MeV for accelerator-driven systems and implementation in MCNPX," *Nucl. Sci. Eng.*, vol. 131, p. 293, 1999.

[3] Y. O. Lee, J. Chang, and M. Kim, "Parameterization and optical model analyses of proton-nucleus cross sections for space shielding," *IEEE Transactions on Nuclear Science*, vol. 47, no. 6, p. 2435, 2000.

[4] Y. O. Lee, T. Fukahori, J. Chang, and S. Chiba, "Optical model potential search for neutron- and proton induced reactions of ^{12}C, ^{16}O, ^{27}Al, ^{56}Fe, ^{90}Zr and ^{208}Pb up to 250 MeV," in *Proc. of PHYSOR 2000: ANS International Topical Meeting on Advances in Reactor Physics and Mathmatics and Computation into the Next Millenium*, Pittsburgh, Pennsylvania, U.S.A, May 7-12, 2000.

[5] M. Meier, D. Clark, C. Goulding, J. Mcclelland, G. Morgan, C. Moss, and W. Amin, "Differential neutron production cross sections and neutron yield from stopping-length targets for 113 MeV," *Nucl. Sci. Eng.*, vol. 102, p. 310, 1989. EXFOR O0100.

[6] M. Meier, W. Amian, C. Goulding, G. Morgan, and C. Moss, "Differential neutron production cross sections for 256-MeV protons," *Nucl. Sci. Eng.*, vol. 110, p. 289, 1992. EXFOR C0168.

[7] W. Scobel, M. Trabandt, M. Blann, B. Pohl, B. Remington, R. Byrd, C. Foster, R. Bonetti, C. Chiesa, and S. Grimes, "Preequilibrium (p,n)reaction as a probe for the effective nucleon-nucleon interaction in multistep direct processes," *Phys. Rev. C*, vol. 41, p. 2010, 1990. EXFOR O0181.

[8] S. Stamer, W. Scobel, W. Amian, R. Byrd, M. Blann, B. Pohl, J. Bisplinghoff, and R. Bonetti, "Double differential cross sections for neutron emission induced by 256 MeV and 800 MeV protons," *Phys. Rev. C*, vol. 47, p. 1647, 1993. EXFOR C0511.

[9] C. Kalbach, "Systematics of continuum angular distributions: Extensions to higher energies," *Phys. Rev. C*, vol. 37, pp. 2350–2370, 1988.

[10] OECD/NEA, "Exfor: Experimental nuclear reaction data retrievals," WWW address: http://www.nea.fr/html/dbdata/x4/welcome.html.

[11] P. G. Young, E. D. Arthur, and M. B. Chadwick, "Comprehensive nuclear model calculations: Theory and use of the GNASH code," in *Proc. of the IAEA Workshop on Nuclear Reaction Data and Nuclear Reactors - Physics, Design, and Safety* (A. Gandini and G. Reffo, eds.), (Singapore), pp. 227–404, Trieste, Italy, April 15 - May 17, 1996, World Scientific Publishing, Ltd., in press.

[12] R. B. Firestone and V. S. Shirley, *Table of Isotopes, 8th edition.* New York, NY: John Wiley and Sons, 1996.

[13] G. Audi and A. Wapstra *Nucl. Phys.*, vol. A595, p. 409, 1995.

[14] P. Moeller, J. Nix, W. Myers, and W. Swiatecki *Atomic Data and Nuclear Data Tables*, vol. 59, p. 185, 1995.

[15] A. V. Ignatyuk, G. N. Smirenkin, and A. Tishin, "Phenomenological description of the energy dependence of the level density parameter," *Sov. J. Nucl. Phys.*, vol. 21, pp. 255–257, 1975.

[16] Y. O. Lee, T. Fukahori, J. Chang, and C. S., "Evaluation of neutron- and proton-induced cross section of Al-27 up to 2 GeV," *J. of Nucl. Sci. and Tech.*, vol. 36, no. 12, p. 1125, 1999.

[17] V. McLane, "ENDF-102 data formats and procedures for the evaluated nuclear data file ENDF-6," Tech. Rep. BNL-NCS-44945, Rev. 2/97, Brookhaven National Laboratory, National Nuclear Data Center, Upton, NY, 1997.

[18] Y. O. Lee and et al., "High energy nuclear data evaluations for neutron-, proton-, and photon-induced reactions at kaeri," in *Proc. of the International Conference on Nuclear Data for Science and Technology*, Oct., Tsukuba, Japan, 2001.